Biochemistry

Article

Cite This: Biochemistry 2018, 57, 4816−4823

pubs.acs.org/biochemistry

A Radical Clock Probe Uncouples H Atom Abstraction from Thioether Cross-Link Formation by the Radical *S*-Adenosyl-L-methionine Enzyme SkfB

William M. Kincannon, Nathan A. Bruender,[†] and Vahe Bandarian*

Department of Chemistry, University of Utah, 315 South 1400 East, Salt Lake City, Utah 84112, United States

Supporting Information

ABSTRACT: Sporulation killing factor (SKF) is a ribosomally synthesized and post-translationally modified peptide (RiPP) produced by *Bacillus*. SKF contains a thioether cross-link between the α-carbon at position 40 and the thiol of Cys32, introduced by a member of the radical *S*-adenosyl-L-methionine (SAM) superfamily, SkfB. Radical SAM enzymes employ a 4Fe−4S cluster to bind and reductively cleave SAM to generate a 5′-deoxyadenosyl radical. SkfB utilizes this radical intermediate to abstract the α-H atom at Met40 to initiate cross-linking. In addition to the cluster that binds SAM, SkfB also has an auxiliary cluster, the function of which is not known. We demonstrate that a substrate analogue with a cyclopropylglycine (CPG) moiety replacing the wild-type Met40 side chain forgoes thioether cross-linking for an alternative radical ring opening of the CPG side chain. The ring opening reaction also takes place with a catalytically inactive SkfB variant in which the auxiliary Fe−S cluster is absent. Therefore, the CPG-containing peptide uncouples H atom abstraction from thioether bond formation, limiting the role of the auxiliary cluster to promoting thioether cross-link formation. CPG proves to be a valuable tool for uncoupling H atom abstraction from peptide modification in RiPP maturases and demonstrates potential to leverage RS enzyme reactivity to create noncanonical amino acids.

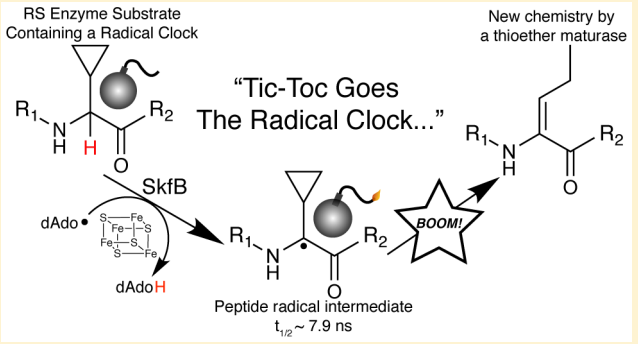

Enzymes in the radical *S*-adenosyl-L-methionine (SAM) superfamily catalyze diverse and often chemically challenging transformations in primary and secondary metabolism. Most radical SAM (RS) enzymes bind a site differentiated 4Fe−4S cluster through thiolate side chains from a CxxxCxxC motif; the fourth iron of the cluster binds SAM through its amino and carboxylate moieties. The role of the RS cluster is to reductively activate SAM for cleavage of one of its C−S bonds,[1−3] in most cases generating a 5′-deoxyadenosyl radical (dAdo•). The dAdo• in turn initiates chemistry by either H atom abstraction or radical addition.[4−6] The radical intermediates that are formed subsequently undergo transformations that result in C−C bond formation, group migration, epimerization, and cross-linking.[4,7]

In addition to the cluster that activates SAM, a growing subset of RS enzymes also harbor additional clusters, termed auxiliary (Aux) clusters.[8,9] Aux clusters are thought to be involved in the enzymatic mechanism and/or in catalytically essential redox transformations.[8−27] In contrast to the role of the RS cluster, the functions of the Aux clusters have remained enigmatic at least partly because their removal destabilizes the proteins.[13,28,29] However, in cases in which it has been possible to remove the Aux cluster(s), overall activity is abolished.[11]

Recent studies have implicated radical SAM enzymes in the maturation of ribosomally encoded and post-translationally modified polypeptides (RiPPs).[30−32] The range of RS-dependent modifications includes cross-linking,[11,14−17,33−35] methylation,[36−44] oxidative decarboxylation,[45−47] epimerization,[43,48−50] and amino acid splicing.[51] Sporulation killing factor (SKF) is an antimicrobial RiPP that is secreted by sporulating *Bacillus subtilis* to lyse and cannibalize non-sporulating neighbors within a colony.[52] The precursor of SKF is encoded by *skfA*, and the thioether cross-link of the mature product is introduced by the RS enzyme SkfB (Scheme 1A). Sequence conservation, biochemical, and spectroscopic investigations of the protein suggest that SkfB harbors at least two clusters, of which the N-terminal cluster bound by the CxxxCxxC motif is necessary for activating SAM. Both are required for thioether bond formation.[33]

The mechanism for SKF thioether cross-link formation is not known, but it was previously reported that SkfB can accommodate various bulky and/or hydrophobic side chains at position 40.[33] In a previous study we exploited this flexibility to incorporate site selective isotopic labels to demonstrate that dAdo• directly abstracts a hydrogen atom from the α-carbon at position 40 and infer the presence of a peptide-based radical.[34]

Received: May 10, 2018
Revised: June 27, 2018
Published: July 2, 2018

DOI: 10.1021/acs.biochem.8b00537
Biochemistry 2018, 57, 4816−4823

Scheme 1. (A) Thioether Formation in SkfA Initiated by H Atom Abstraction at the Cα Atom of Met40 by SkfB and (B) Radical Ring Opening Catalyzed by SkfB with CPG-Containing SkfA

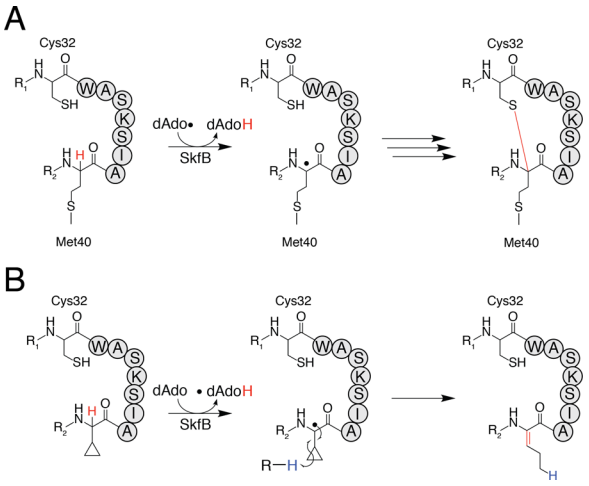

This finding, in combination with the promiscuity of the enzyme, suggested that we could further exploit SkfB not only to interrogate the H atom abstraction step but also to determine if the Aux plays any role in this process.

Because of their propensity of rapid ring opening to a homoallylic radical, cyclopropyl moieties have been used as diagnostic probes for radical intermediates in enzymatic transformations.[53−64] For example, the isopropyl cyclopropane radical undergoes ring opening at a rate of 8.8×10^7 s^{-1}.[65] The inclusion of a cyclopropyl moiety at the site of H atom abstraction in SkfA would permit one to examine partitioning between ring opening and thioether bond formation. Herein, we report that SkfB catalyzes ring opening of cyclopropylglycine-bearing SkfA, providing unambiguous evidence of generation of a radical intermediate. Moreover, a catalytically inactive SkfB variant that lacks the auxiliary cluster is shown to perform the same transformation allowing uncoupling of H atom abstraction from thioether cross-linking in SkfB.

MATERIALS AND METHODS

Cloning and Expression of ΔAux SkfB. The *skfB* gene was previously amplified via polymerase chain reaction from the *Bacillus subtilis* subsp. subtilis str 168 genome and cloned into a pET28JT[66] vector, with the resulting construct named pNB529.[34] The ΔAux variant (pNB611) was generated by consecutive site-directed mutageneses, using the primers listed in Table S1. First, pNB606, a C351A variant, was generated using the pNB529 plasmid as a template. Then, pNB611, a C351A/C385A double mutant variant, was generated using the pNB606 plasmid as a template. Standard Sanger sequencing at the University of Michigan DNA Sequencing Core confirmed the sequence of each construct. The variants were expressed and purified as discussed previously.[34]

Elemental Analysis. The iron contents of wild-type (WT) and ΔAux SkfB were determined by ICP-OES. Concentrated SkfB and ΔAux SkfB were diluted to 1 μM (based on the corrected Bradford concentration)[34] in 1% (v/v) trace-metal grade nitric acid. Analyses were conducted by the Analytical Facilities of the Department of Hydrology & Atmospheric Sciences at the University of Arizona. The acid-labile sulfide content of SkfB (wild type and ΔAux) was determined using the Beinert method.[67]

Peptide Synthesis. A PS3 peptide synthesizer (Protein Technologies Inc.) was used to synthesize wild-type SkfA, CPG-SkfA, SIAXTR, and SIAZ′TR on a 0.025 mmol scale by a solid phase peptide synthesis methodology, as discussed previously.[34] Fmoc-L-cyclopropylglycine and Fmoc-L-norvaline were purchased from ChemImpex. All other protected Fmoc-L-amino acids were purchased from Protein Technologies Inc. Following synthesis and cleavage from resin, the peptide was resuspended in water and lyophilized to dryness.

Purification of Synthetic Peptides. Each crude peptide was purified by HPLC using a Phenomenex Jupiter C12 prep column (21.2 mm × 250 mm, 4 μm particle size, 90 Å pore size). The HPLC method for purification and the method for LC−MS analysis of fractions have been discussed previously.[34] The fractions containing pure peptide were pooled and lyophilized to dryness.

Analysis of the Purity of the Synthetic Peptide. SkfA peptide fractions were analyzed for purity using a LTQ-OrbiTrap XL instrument (Thermo Fisher) connected to a Vanquish UHPLC instrument (Thermo Fisher) with a diode array detector by injecting an aliquot onto a Hypersil GOLD C4 column (2.1 mm × 150 mm, 1.9 μm particle size; Thermo Fisher) pre-equilibrated in 95% buffer A and 5% buffer B. Buffer A consisted of 0.1% (v/v) LC−MS Optima TFA (Fisher) in LC−MS Optima water (Fisher). Buffer B consisted of 0.1% (v/v) LC−MS Optima TFA (Fisher) in LC−MS Optima acetonitrile (Fisher). The SIAXTR and SIAZ′TR peptide fractions were analyzed for purity also by UHPLC−MS, but with a Hypersil GOLD C18 column (2.1 mm × 150 mm, 1.9 μm particle size; Thermo Fisher) pre-equilibrated in 95% buffer A and 5% buffer B. Buffer A consisted of 0.1% (v/v) LC−MS Optima TFA (Fisher) in LC−MS Optima water (Fisher). Buffer B consisted of 0.1% (v/v) LC−MS Optima TFA (Fisher) in LC−MS Optima acetonitrile (Fisher). The buffer compositions were the same as those used for the C4 column. For both columns, the reaction components were eluted at a rate of 0.2 mL/min with the following program: 5% B from 0 to 1 min, 5 to 70% B from 1 to 11.5 min, 70 to 100% B from 11.5 to 11.6 min, 100% B from 11.6 to 16.6 min, 100 to 5% B from 16.6 to 16.7 min, and 5% B from 16.7 to 21.7 min. All data were analyzed in Xcalibur (Thermo Fisher). Chromatogram profiles were smoothed with a boxcar algorithm set to a value of 5. The deconvoluted spectra of SkfA were generated from the raw LC−MS data using the Xtract software (Thermo Fisher).

Analysis of the Thioether and Deuterium Content of SkfA and CPG-SkfA upon Incubation with SkfB. Reactions of SkfB with wild-type SkfA or CPG-SkfA were conducted in an anoxic environment (Coy Laboratories anaerobic chamber with a 97% N_2/3% H_2 atmosphere) and analyzed by UHPLC−MS to examine the deuterium content of both. Reaction mixtures in ^2H_2O (99.9%, Cambridge Isotope Laboratories, Inc.) contained 0.05 M Tris-^{2}HCl (p^{2}H 8.0), 0.01 M DTT, 0.1 M KCl, 2 mM SAM, 1 mM dithionite, 0.1 mg of SkfA, and 0.05 mM SkfB, in a final volume of 0.1 mL. The buffer p^{2}H was adjusted with ^{2}HCl (99.5%, Cambridge Isotope Laboratories, Inc.). Salts were dissolved in 99.9% ^2H_2O prior to addition. The peptide was H/D exchanged by repeated rounds (at least three) of washes in ^2H_2O, followed by lyophilization. After hydrogen/deuterium exchange, the peptide was resuspended in 0.05 M Tris-^{2}HCl (pD 8.0) and

DOI: 10.1021/acs.biochem.8b00537
Biochemistry 2018, 57, 4816−4823

0.01 M DTT to a concentration of 10 g L^{-1}. The enzymes were exchanged into ^2H_2O by repeated rounds of concentration and dilution in an Amicon concentrator fitted with YM-10 membranes in the anaerobic chamber. A 0.1 mL aliquot of the concentrated enzyme was diluted to 1 mL with 0.05 M Tris-^{2}HCl (p^2H 8.0), 0.01 M DTT, and 0.15 M KCl and subsequently concentrated to the starting volume. This was repeated at least three times.

The reaction was initiated by addition of substrate, and the mixture was incubated at room temperature overnight. The next day, the reaction mixture was treated with 2 μL of 1 M iodoacetamide to alkylate all free Cys thiolates in the SkfA peptide. The alkylation reaction mixture was incubated at room temperature in the dark for 30 min, and the reaction was subsequently quenched with 10 μL of 30% (w/v) trichloroacetic acid. The quenched samples were centrifuged at 16000*g* for 10 min to pellet the insoluble material. The soluble portion was frozen, lyophilized, and subsequently washed with H_2O several times for hydrogen/deuterium exchange. After at least three cycles, the peptide was resuspended in 0.1 mL of H_2O. The SAM was enzymatically synthesized and purified as described previously.[68]

The SkfA peptides were analyzed for thioether cross-link formation and deuterium content using a LTQ-OrbiTrap XL instrument (Thermo Fisher) connected to a Vanquish UHPLC instrument (Thermo Fisher) and a diode array detector. An aliquot was injected onto a Hypersil GOLD C4 column (2.1 mm × 150 mm, 1.9 μm particle size; Thermo Fisher) pre-equilibrated in 95% buffer A and 5% buffer B. Buffer A consisted of 0.1% (v/v) LC−MS Optima TFA (Fisher) in LC−MS Optima water (Fisher). Buffer B consisted of 0.1% (v/v) LC−MS Optima TFA (Fisher) in LC−MS Optima acetonitrile (Fisher). The reaction components were eluted at a rate of 0.2 mL/min with the following program: 5% B from 0 to 1 min, 5 to 70% B from 1 to 11.5 min, 70 to 100% B from 11.5 to 11.6 min, 100% B from 11.6 to 16.6 min, 100 to 5% B from 16.6 to 16.7 min, and 5% B from 16.7 to 21.7 min. All data were analyzed in Xcalibur (Thermo Fisher). The deconvoluted spectra of SkfA were generated from the raw LC−MS data using the Xtract software (Thermo Fisher).

Analysis of the Deuterium Content of Tryptic Digests of CPG-SkfA following Incubation with SkfB. Reactions were conducted the same as described above. Following TCA precipitation and hydrogen/deuterium exchange, the extracted peptides were resuspended in 50 mM Tris-HCl (pH 8.0) containing 0.5 mM $CaCl_2$. Bovine pancreatic trypsin (Sigma) was added to each extract [1:100 trypsin:peptide weight ratio (milligrams)]. The trypsin reaction mixtures were incubated for 6 h at 37 °C. The digested peptide was passed through a YM-10 membrane (VWR) via centrifugation at 10000*g* for 10 min.

The CPG-SkfA tryptic fragments were analyzed for deuterium content using a LTQ-OrbiTrap XL instrument (Thermo Fisher) connected to a Vanquish UHPLC instrument (Thermo Fisher) with a diode array detector by injecting an aliquot onto a Hypersil GOLD C18 column (2.1 mm × 150 mm, 1.9 μm particle size; Thermo Fisher) pre-equilibrated in 95% buffer A and 5% buffer B. Buffer A consisted of 0.1% (v/v) LC−MS Optima TFA (Fisher) in LC−MS Optima water (Fisher). Buffer B consisted of 0.1% (v/v) LC−MS Optima TFA (Fisher) in LC−MS Optima acetonitrile (Fisher). The reaction components were eluted at a rate of 0.2 mL/min with the following program: 0% B from 0 to 1 min, 0 to 70% B from 1 to 11.5 min, 70 to 100% B from 11.5 to 11.6 min, 100% B from 11.6 to 20 min, 100 to 0% B from 20 to 20.1 min, and 0% B from 20.1 to 23.1 min. All data were analyzed in Xcalibur (Thermo Fisher). Chromatogram profiles were smoothed with a boxcar algorithm set to a value of 5.

MS/MS Analysis of CPG-SkfA Tryptic Fragments. Reactions, tryptic digestions, and UHPLC methods were the same as those described above. The peak corresponding to the +1 charge state of the unmodified or modified SIAXTR tryptic fragment were isolated in the CID cell using an isolation width of m/z 0.5, a Q of 0.25, an activation time of 30 ms, and a collision energy of 28%. The MS/MS experiments were carried out using the FT analyzer set to a resolution of 100000, one microscan, and a 200 ms maximum injection time. The CID experiment for detecting the unmodified peptide began 6.6 min after injection of the sample onto the C18 column and continued for 1.05 min. The CID experiment for detecting the modified peptide began 6.96 min after UHPLC injection and continued for 2.10 min. Predicted isotope distributions for deuterium-incorporated peptide were calculated using Scientific Instrument Services (SIS) Isotope Distribution Calculator and Mass Spec Plotter (http://www.sisweb.com/mstools/isotope.htm).

Analysis of 5′-Deoxyadenosine Production by SkfB Variants. To determine if the CPG substrate analogue effectively mimics the reactivity of the native substrate, assays were conducted to monitor the amount of *S*-adenosyl-L-methionine reductively cleaved to form 5′-deoxyadenosine by WT and ΔAux SkfB. The assay conditions were the same as described above, except that 20 μM enzyme was used and the total reaction volume was 0.25 mL. After the reaction had been initiated with the addition of SAM, aliquots of 0.03 mL were removed at 5, 15, 30, 60, and 120 min and the reactions were quenched by combining the mixtures with 0.03 mL of 30% (w/v) TCA. Insoluble material was removed by centrifugation, and an aliquot (25 μL) was analyzed using a Hypersil GOLD C18 column (2.1 mm × 150 mm, 1.9 μm particle size; Thermo Fisher) attached to a Thermo Scientific Dionex UltiMate 3000 UHPLC instrument. The column was pre-equilibrated in 100% buffer A. Buffer A consisted of 50 mM ammonium acetate (Fisher) in LC−MS Optima water. Buffer B consisted of 60% (v/v) LC−MS Optima acetonitrile (Fisher) and 40% LC−MS water (Fisher). The reaction components were eluted at a rate of 0.2 mL/min with the following program: 0% B from 0 to 3.46 min, 0 to 0.9% B from 3.46 to 3.69 min, 0.9 to 1.5% B from 3.69 to 3.92 min, 1.5 to 3% B from 3.92 to 4.25 min, 3 to 20% B from 4.25 to 6.5 min, 20 to 25% B from 6.5 to 7 min, 25 to 40% B from 7 to 8.5 min, 40 to 45% B from 8.5 to 9.25 min, 45 to 60% B from 9.25 to 9.95 min, 60 to 100% B from 9.95 to 10.45 min, 100% B from 10.45 to 16 min, 100 to 0% B from 16 to 16.1 min, and 0% B from 16.1 to 20 min. The peak corresponding to 5′-deoxyadenosine was integrated and quantified using a standard curve created from authentic 5′-deoxyadenosine.[34,69]

RESULTS AND DISCUSSION

To probe the mechanism of SkfB, an SkfA variant in which M40 is replaced with a cyclopropylglycine (CPG) was prepared by solid phase peptide synthesis, purified by preparative HPLC, and analyzed by high-resolution mass spectrometry (HRMS). The mass spectrum of the pure peptide reveals $[M + H]^+$ of 5765.9984 for the peptide,

DOI: 10.1021/acs.biochem.8b00537
Biochemistry 2018, 57, 4816−4823

which is within 0.2 ppm of that expected for M40CPG-SkfA (Figure S1).

The formation of a thioether cross-link in SkfA catalyzed by SkfB is accompanied by a 2 amu decrease in the mass of SkfA, or a 57 amu decrease when the product is carbamidomethylated.[33,34] In contrast to the WT peptide, which clearly exhibits the expected mass shifts across all charge envelopes when SkfB is present (Figure S2), peaks for cross-linked species fail to develop when the CPG-containing SkfA is incubated with SkfB (Figure S3). Therefore, CPG-SkfA does not appear to be a substrate for thioether cross-linking by SkfB, even though the relative amounts of 5′-deoxyadenosine produced by SkfB upon its incubation with CPG-SkfA are comparable to those that are observed with WT SkfA (Figure S4). However, a cyclopropane ring opening and quenching of the subsequent peptide-based radical by H atom abstraction would lead to a product that is isobaric with the starting CPG-SkfA substrate (Scheme 1B).

To determine if reaction with CPG-SkfA occurs, we performed the incubations of CPG-SkfA with SkfB in ^2H_2O. In these experiments, all reagents were extensively exchanged with ^2H_2O (see Materials and Methods for details). Control experiments show that when the reactions with WT SkfA are performed in ^2H_2O, the thioether-containing product has the same mass as that obtained when the reaction is performed in H_2O (Figure S5). By contrast, when CPG-SkfA is incubated with SkfB in ^2H_2O, mass spectral features of the peptide are altered in a predictable manner (Figure 1A and Figure S6). Upon careful examination of the spectral envelopes, distinct changes in intensities of the isotope peaks are seen (Figure 1B), which are quantified as follows.

Using the peak at m/z 1485.7594 as the reference, the intensities of all peaks at lower m/z values decrease and those at higher m/z values increase, therefore indicating an overall increase in m/z for the species. Consistent with this observation, the mass calculated for the product upon deconvolution of the full mass spectrum is 1.0039 amu greater when the reactions are performed in ^2H_2O (Figure 1C).

To establish the location of the ^2H, the product was subjected to trypsin digestion and the resulting peptides were analyzed by LC−MS. Control experiments, in which the unmodified CPG-SkfA is digested with trypsin, yield the hexapeptide (SIAXTR, where X = CPG).

The extracted ion chromatograms (EICs) at m/z 644 and 645, which correspond to the monoisotopic and natural abundance ^{13}C isotope, respectively, both show a peak at 6.9 min (Figure 2A,B, black). The corresponding spectral envelope for the peptide (Figure 2C, black) is consistent with $[M + H]^+$ of the hexapeptide.

After incubation of CPG-SkfA with SkfB in ^2H_2O and tryptic proteolysis, we observe the same peak in the EIC at m/z 644, corresponding to the unmodified peptide. However, at m/z 645, we observe two peaks with distinct retention times (Figure 2B, red). The unmodified peptide is expected to have a peak at m/z 645, which corresponds to the natural abundance ^{13}C isotope (compare to Figure 2B, black). The second peak that is present in the chromatogram appears to have a distinct retention time of 7.2 min, suggesting that it is structurally distinct from the CPG-bearing fragment. The MS spectrum of the species eluting at 7.2 min clearly shows a peak at m/z 645.3767 (Figure 2C, red), which is consistent with a ring-opened product that has incorporated a single, nonexchangeable ^2H (SIAZTR, where Z = ring open CPG).

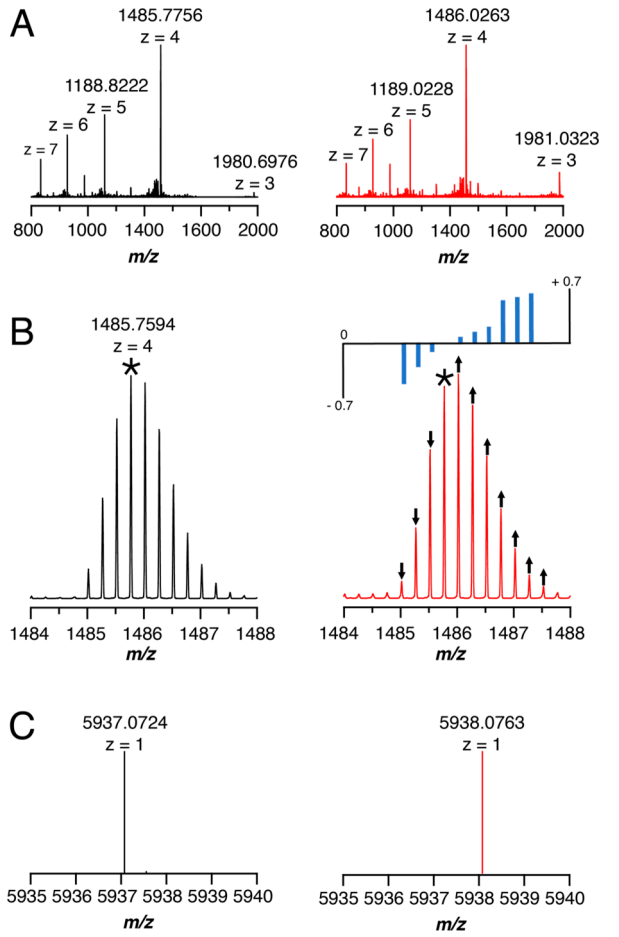

Figure 1. (A) Full mass spectra of CPG-SkfA incubated in the absence (black) or presence (red) of SkfB and carbamidomethylated after incubation. (B) The +4 charge state envelopes from the mass spectra in panel A are shown. The asterisk marks the average m/z of the unreacted peptide (black). Peaks with increased intensity relative the intensity of this peak are shown with up arrows, while lower m/z peaks are shown with down arrows. The changes are shown visually in the bar graph above the red trace. (C) Deconvoluted mass spectra of the samples from panel A showing the calculated $[M + H]^+$ for CPG-SkfA after iodoacetamide treatment.

More significantly, the peak at m/z 645.3767 is much larger than would be expected from the isotopic contribution from natural abundance ^{13}C from the unmodified peptide, which is only consistent with the assignment of this peak as a singly deuterated peptide. The formation of the deuterated species is dependent upon the presence of the enzyme, substrate, reductant, and SAM (Figure S7). We also observe a shoulder in the EIC at m/z 644, which has the retention time of the ring-opened product. This peak could arise from residual ^1H and/or quenching of a small portion of the radical intermediate from a site that cannot be solvent exchanged. Note that this peak is absent when enzyme is omitted (compare red and black traces in Figure 2).

Two hexapeptides were synthesized to validate the differences in the retention times of the CPG and ring-opened product. The sequences of these products are SIAXTR and SIAZ′TR, the second being a close structural analogue that incorporated norvaline instead of Z (Figures S8 and S9). When the two peptides are co-injected, the analogues have the same separation seen in the tryptic digests (Figure S10).

DOI: 10.1021/acs.biochem.8b00537
Biochemistry 2018, 57, 4816−4823

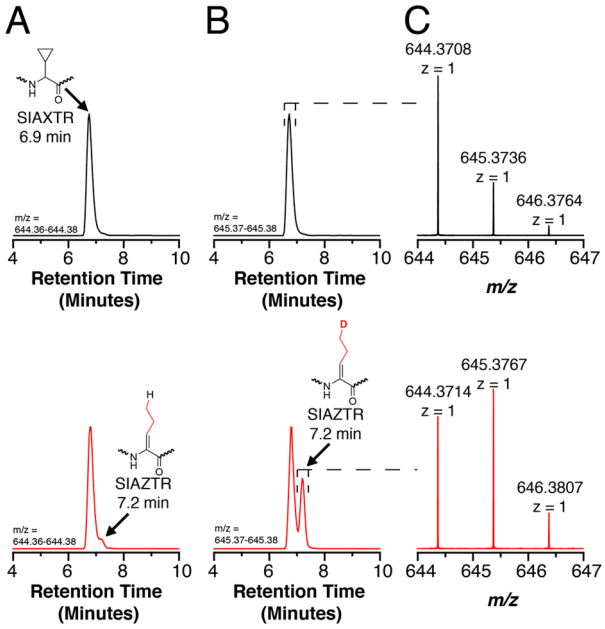

Figure 2. EIC and mass spectra of CPG-containing hexapeptide trypsin digest fragments of CPG-SkfA. The top panels correspond to CPG-SkfA with no SkfB prior to trypsin treatment (black traces), while the bottom panels correspond to CPG-SkfA incubated with SkfB prior to trypsin treatment (red traces). (A) EIC for the peak at m/z 644.36−644.38 and (B) EIC for the peak at m/z 645.37−645.38. Via comparison of the black and red traces, a new peak appears upon reaction with SkfB. One is assigned as the starting material, and the new peak with a longer retention time corresponds to a new product with a ^{2}H incorporated. Chemical structures of the proposed substrate and product are shown in panel A, with D representing ^{2}H. (C) Mass spectrum from m/z 644 to 647 of two species found and highlighted in panel B. The new peak shows that the hexapeptide from the enzyme incubation shows an increased intensity at m/z 645.38 compared to the unreacted form.

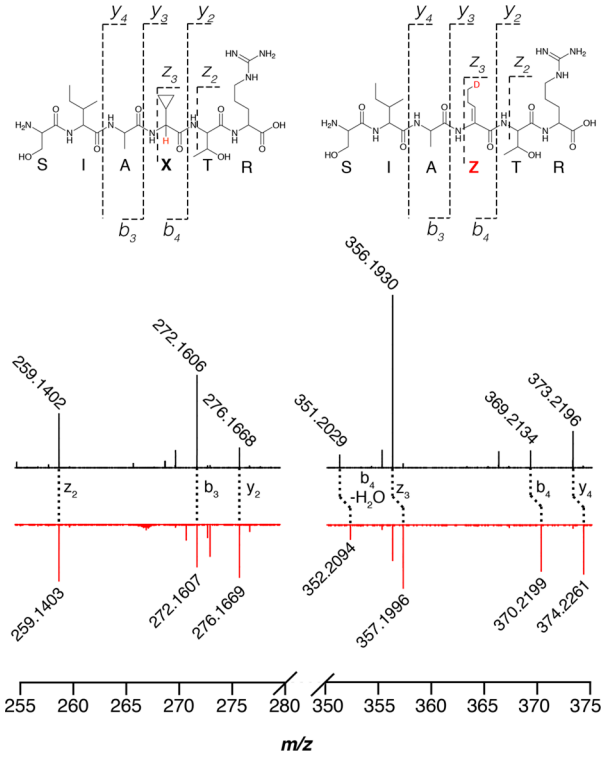

Figure 3. MS/MS spectra of the tryptic hexapeptides of CPG-SkfA that has been incubated in ^2H_2O in the absence (black) and presence (red) of SkfB. The observed y, b, and z ions are indicated in the corresponding structures. Fragments containing the CPG residue are shifted by 1 amu upon being incubated with SkfB, while fragments that do not contain the CPG residue have the same m/z values as when the enzyme is omitted (see the dotted lines connecting the black and red traces).

To further probe the position of the ^{2}H, we performed MS/MS analysis. The species with peaks at m/z 644.37 and 645.38 corresponding to SIAXTR and SIAZTR, respectively, were fragmented in the CID cell of the LTQ-Orbitrap instrument, and the corresponding fragments were analyzed in the Orbitrap detector. The incorporation of ^{2}H at position 40 is unambiguously demonstrated by the MS/MS data (compare spectra in Figure 3). Specifically, we observe shifts in the masses of the fragments containing the CPG-based product, such as z_3, y_4, and b_4 fragments in Figure 3, when CPG-SkfA is incubated with the enzyme in ^2H_2O. A complete list of observed fragments appears in Table S3.

The observation that SkfB catalyzes ring opening in the CPG-bearing peptide without forming a thioether cross-link suggests that the lifetime of the activated radical clock is much shorter than that of turnover. This ultrafast substrate provides an opportunity to determine if the Aux cluster is at all required for the H atom abstraction step. Note that the Aux cluster is necessary for thioether formation but not for reductive cleavage of SAM.[33] Beyond this observation, little else is known about the role of Aux clusters in peptide maturases, but it has been suggested that the cluster may serve as a binding site for the substrate.[8−11,14] To explore the potential role of the Aux cluster, we prepared an SkfB variant in which the highly conserved residues that are putative ligands to Aux (C351 and C385) are mutated to Ala to obtain the ΔAux variant. These residues were selected on the basis of their conservation outside the CxxxCxxC motif that binds the radical SAM cluster (Figure S11).

ΔAux-SkfB is purified by affinity chromatography, followed by removal of the N-terminal affinity tag with TEV protease, and reconstituted with Fe/S as described for the WT protein.[34] Fe/S analysis of WT SkfB indicates the presence of 8.1 and 6.2 mol of Fe and S, respectively. In the ΔAux variant, these are reduced to 4.6 and 4.5, respectively, consistent with the loss of the cluster (Table S2).

Incubation of the ΔAux variant with SkfA does not lead to formation of any cross-links (Figure S2), as has been observed previously.[33] However, when CPG-SkfA is used in ^2H_2O, under the same conditions as with the WT enzyme, we observe incorporation of deuterium into the peptide (Figure S6), which we further localize to the SIAZTR trypsin fragment (Figure S7).

The ability of ΔAux-SkfB to catalyze ring opening in CPG-SkfA is highly suggestive that the Aux cluster is not required for the initial H atom abstraction. This result has broad implications for radical SAM enzymes. Specifically, it can now be stated that *a priori*, there is no need for an Aux cluster in H atom abstraction from the substrate. On the basis of our data, we suggest that the Aux cluster is required by SkfB only for promoting the formation of the thioether after the initial H atom abstraction, presumably by acting in redox capacity, or in positioning the peptide for the optimal cross-linking geometry. We note that a role for the Aux cluster in binding the substrate

DOI: 10.1021/acs.biochem.8b00537
Biochemistry 2018, 57, 4816−4823

and potentially in redox has been suggested for thioether cross-link-forming enzymes, such as AlbA,[14] CteB,[10] and Tte.[11] The exact role of the auxiliary cluster, however, remains to be established.

Cyclopropylcarbinyl radicals are termed radical clocks because of their well-known propensity for rapid ring opening to a homoallylic radical.[65] While we cannot rule out the possibility that the environment of the active site and the nature of the intermediate influences the rate of ring opening relative to those of the nonenzymatic systems, rates of ring opening of a wide array of substituted cyclopropane derivatives, such as the isopropyl cyclopropane, suggest that the half-life of the initially formed radical is at least 7.9 ns.[65] Our observation of the cyclopropyl glycine ring opening is the first direct insight into the lifetime of a radical species in the active site of a radical SAM enzyme.

There is currently significant interest in leveraging the RiPP maturase biosynthetic logic toward synthesis of peptides with novel amino acids. To the extent that a radical SAM maturase can tolerate substitution of CPG, it may be possible to use SkfB or similar maturases to generate a dehydronorvaline-like side chain. From a mechanistic perspective, the incorporation of CPG into radical SAM RiPP maturases, where tolerated, provides a powerful tool for uncoupling the overall reaction from the initial H atom abstraction step. To the best of our knowledge, an uncoupled C−H cleavage has been observed only with the RS enzyme DesII using catalytically inactive fluorinated analogues of the substrate.[70] However, CPG-SkfA is the first instance of a substrate that uncouples H-atom abstraction from overall turnover in a RS RiPP maturase. If it were possible to tune sequence preference, CPG may provide a method to unmask, at will, new amino acid functional groups.

■ ASSOCIATED CONTENT

Supporting Information

The Supporting Information is available free of charge on the ACS Publications website at DOI: 10.1021/acs.biochem.8b00537.

Tables S1−S3 and Figures S1−S10 (PDF)

■ AUTHOR INFORMATION

Corresponding Author

*E-mail: vahe@chem.utah.edu.

ORCID

Nathan A. Bruender: 0000-0002-6129-8897

Vahe Bandarian: 0000-0003-2302-0277

Present Address

†N.A.B.: Department of Chemistry and Biochemistry, St. Cloud State University, St. Cloud, MN 56301.

Funding

The work reported in this publication was supported by National Institutes of General Medical Sciences Grants GM72623 and GM120638.

Notes

The authors declare no competing financial interest.

■ ABBREVIATIONS

CID, collision-induced dissociation; CPG, cyclopropylglycine; DTT, dithiothreitol; FMOC, fluorenylmethyloxycarbonyl; HPLC, high-performance liquid chromatography; LC−MS, liquid chromatography−mass spectrometry; SAM, *S*-adenosyl-L-methionine; SDS−PAGE, sodium dodecyl sulfate−polyacrylamide gel electrophoresis; Tris, tris(hydroxymethyl)-aminomethane; UHPLC−MS, ultra-high-performance liquid chromatography−mass spectrometry.

■ REFERENCES

(1) Sofia, H. J., Chen, G., Hetzler, B. G., Reyes-Spindola, J.F., and Miller, N. E. (2001) Radical SAM, a novel protein superfamily linking unresolved steps in familiar biosynthetic pathways with radical mechanisms: functional characterization using new analysis and information visualization methods. *Nucleic Acids Res. 29*, 1097−1106.

(2) Krebs, C., Broderick, W. E., Henshaw, T. F., Broderick, J. B., and Huynh, B. H. (2002) Coordination of adenosylmethionine to a unique iron site of the [4Fe-4S] of pyruvate formate-lyase activating enzyme: A Mossbauer spectroscopic study. *J. Am. Chem. Soc. 124*, 912−913.

(3) Chen, D., Walsby, C., Hoffman, B. M., and Frey, P. A. (2003) Coordination and mechanism of reversible cleavage of S-adenosylmethionine by the [4Fe-4S] center in lysine 2,3-aminomutase. *J. Am. Chem. Soc. 125*, 11788−11789.

(4) Bauerle, M. R., Schwalm, E. L., and Booker, S. J. (2015) Mechanistic diversity of radical S-adenosylmethionine (SAM)-dependent methylation. *J. Biol. Chem. 290*, 3995−4002.

(5) Mahanta, N., Fedoseyenko, D., Dairi, T., and Begley, T. P. (2013) Menaquinone biosynthesis: Formation of aminofutalosine requires a unique radical SAM enzyme. *J. Am. Chem. Soc. 135*, 15318−15321.

(6) Lilla, E. A., and Yokoyama, K. (2016) Carbon extension in peptidylnucleoside biosynthesis by radical-SAM enzymes. *Nat. Chem. Biol. 12*, 905−907.

(7) Broderick, J. B., Duffus, B. R., Duschene, K. S., and Shepard, E. M. (2014) Radical S-adenosylmethionine enzymes. *Chem. Rev. 114*, 4229−4317.

(8) Lanz, N. D., and Booker, S. J. (2015) Auxiliary iron-sulfur cofactors in radical SAM enzymes. *Biochim. Biophys. Acta, Mol. Cell Res. 1853*, 1316−1334.

(9) Grell, T. A. J., Goldman, P. J., and Drennan, C. L. (2015) SPASM and Twitch domains in S-Adenosylmethionine (SAM) radical enzymes. *J. Biol. Chem. 290*, 3964−3971.

(10) Grove, T. L., Himes, P. M., Hwang, S., Yumerefendi, H., Bonanno, J. B., Kuhlman, B., Almo, S. C., and Bowers, A. A. (2017) Structural Insights into Thioether Bond Formation in the Biosynthesis of Sactipeptides. *J. Am. Chem. Soc. 139*, 11734−11744.

(11) Bruender, N. A., Wilcoxen, J., Britt, R. D., and Bandarian, V. (2016) Biochemical and Spectroscopic Characterization of a Radical S-Adenosyl- l -methionine Enzyme Involved in the Formation of a Peptide Thioether Cross-Link. *Biochemistry 55*, 2122−2134.

(12) Goldman, P. J., Grove, T. L., Sites, L. A., McLaughlin, M. I., Booker, S. J., and Drennan, C. L. (2013) X-ray structure of an AdoMet radical activase reveals an anaerobic solution for formylglycine posttranslational modification. *Proc. Natl. Acad. Sci. U. S. A. 110*, 8519−8524.

(13) Saichana, N., Tanizawa, K., Ueno, H., Pechoušek, J., Novák, P., and Frébortová, J. (2017) Characterization of auxiliary iron−sulfur clusters in a radical S-adenosylmethionine enzyme PqqE from Methylobacterium extorquens AM1. *FEBS Open Bio 7*, 1864−1879.

(14) Flühe, L., Knappe, T. A., Gattner, M. J., Schäfer, A., Burghaus, O., Linne, U., and Marahiel, M. A. (2012) The radical SAM enzyme AlbA catalyzes thioether bond formation in subtilosin A. *Nat. Chem. Biol. 8*, 350−357.

(15) Benjdia, A., Decamps, L., Guillot, A., Kubiak, X., Ruffié, P., Sandström, C., and Berteau, O. (2017) Insights into the catalysis of a lysine-tryptophan bond in bacterial peptides by a SPASM domain radical S-adenosylmethionine (SAM) peptide cyclase. *J. Biol. Chem. 292*, 10835−10844.

(16) Schramma, K. R., Forneris, C. C., Caruso, A., and Seyedsayamdost, M. R. (2018) Mechanistic Investigations of

DOI: 10.1021/acs.biochem.8b00537
Biochemistry 2018, 57, 4816−4823

Lysine-Tryptophan Crosslink Formation Catalyzed by Streptococcal Radical SAM Enzymes. *Biochemistry 57*, 461.
(17) Davis, K. M., Schramma, K. R., Hansen, W. A., Bacik, J. P., Khare, S. D., Seyedsayamdost, M. R., and Ando, N. (2017) Structures of the peptide-modifying radical SAM enzyme SuiB elucidate the basis of substrate recognition. *Proc. Natl. Acad. Sci. U. S. A. 114*, 10420−10425.
(18) Maiocco, S. J., Grove, T. L., Booker, S. J., and Elliott, S. J. (2015) Electrochemical Resolution of the [4Fe-4S] Centers of the AdoMet Radical Enzyme BtrN: Evidence of Proton Coupling and an Unusual, Low-Potential Auxiliary Cluster. *J. Am. Chem. Soc. 137*, 8664−8667.
(19) McLaughlin, M. I., Lanz, N. D., Goldman, P. J., Lee, K.-H., Booker, S. J., and Drennan, C. L. (2016) Crystallographic snapshots of sulfur insertion by lipoyl synthase. *Proc. Natl. Acad. Sci. U. S. A. 113*, 9446−9450.
(20) Suess, D. L. M., Pham, C. C., Bürstel, I., Swartz, J. R., Cramer, S. P., and Britt, R. D. (2016) The Radical SAM Enzyme HydG Requires Cysteine and a Dangler Iron for Generating an Organometallic Precursor to the [FeFe]-Hydrogenase H-Cluster. *J. Am. Chem. Soc. 138*, 1146−1149.
(21) Mulliez, E., Duarte, V., Arragain, S., Fontecave, M., and Atta, M. (2017) On the Role of Additional [4Fe-4S] Clusters with a Free Coordination Site in Radical-SAM Enzymes. *Front. Chem. 5*, 1−13.
(22) Dinis, P., Suess, D. L. M., Fox, S. J., Harmer, J. E., Driesener, R. C., De La Paz, L., Swartz, J. R., Essex, J. W., Britt, R. D., and Roach, P. L. (2015) X-ray crystallographic and EPR spectroscopic analysis of HydG, a maturase in [FeFe]-hydrogenase H-cluster assembly. *Proc. Natl. Acad. Sci. U. S. A. 112*, 1362−1367.
(23) Kühner, M., Schweyen, P., Hoffmann, M., Ramos, J. V., Reijerse, E. J., Lubitz, W., Bröring, M., and Layer, G. (2016) The auxiliary [4Fe−4S] cluster of the Radical SAM heme synthase from Methanosarcina barkeri is involved in electron transfer. *Chem. Sci. 7*, 4633−4643.
(24) Ruszczycky, M. W., and Liu, H. W. (2015) Mechanistic enzymology of the radical SAM enzyme DesII. *Isr. J. Chem. 55*, 315−324.
(25) Perche-Letuvée, P., Kathirvelu, V., Berggren, G., Clemancey, M., Latour, J. M., Maurel, V., Douki, T., Armengaud, J., Mulliez, E., Fontecave, M., Garcia-Serres, R., Gambarelli, S., and Atta, M. (2012) 4-Demethylwyosine synthase from Pyrococcus abyssi is a radical-S-adenosyl- L-methionine enzyme with an additional [4FE-4S]+2cluster that interacts with the pyruvate Co-substrate. *J. Biol. Chem. 287*, 41174−41185.
(26) Kathirvelu, V., Perche-Letuvée, P., Latour, J.-M., Atta, M., Forouhar, F., Gambarelli, S., and Garcia-Serres, R. (2017) Spectroscopic evidence for cofactor−substrate interaction in the radical-SAM enzyme TYW1. *Dalt. Trans. 46*, 13211−13219.
(27) Hanzelmann, P., and Schindelin, H. (2006) Binding of 5′-GTP to the C-terminal FeS cluster of the radical S-adenosylmethionine enzyme MoaA provides insights into its mechanism. *Proc. Natl. Acad. Sci. U. S. A. 103*, 6829−6834.
(28) Boss, L., Oehme, R., Billig, S., Birkemeyer, C., and Layer, G. (2017) The Radical SAM enzyme NirJ catalyzes the removal of two propionate side chains during heme d_1 biosynthesis. *FEBS J. 284*, 4314−4327.
(29) Barr, I., Stich, T. A., Gizzi, A. S., Grove, T. L., Bonanno, J. B., Latham, J. A., Chung, T., Wilmot, C. M., Britt, R. D., Almo, S. C., and Klinman, J. P. (2018) X-ray and EPR Characterization of the Auxiliary Fe−S Clusters in the Radical SAM Enzyme PqqE. *Biochemistry 57*, 1306−1315.
(30) Ortega, M. A., and Van Der Donk, W. A. (2016) New Insights into the Biosynthetic Logic of Ribosomally Synthesized and Post-translationally Modified Peptide Natural Products. *Cell Chem. Biol. 23*, 31−44.
(31) Latham, J. A., Barr, I., and Klinman, J. P. (2017) At the confluence of ribosomally synthesized peptide modification and radical S-adenosylmethionine (SAM) enzymology. *J. Biol. Chem. 292*, 16397−16405.
(32) Mahanta, N., Hudson, G. A., and Mitchell, D. A. (2017) Radical S-Adenosylmethionine Enzymes Involved in RiPP Biosynthesis. *Biochemistry 56*, 5229−5244.
(33) Flühe, L., Burghaus, O., Wieckowski, B. M., Giessen, T. W., Linne, U., and Marahiel, M. A. (2013) Two [4Fe-4S] clusters containing radical SAM enzyme SkfB catalyze thioether bond formation during the maturation of the sporulation killing factor. *J. Am. Chem. Soc. 135*, 959−962.
(34) Bruender, N. A., and Bandarian, V. (2016) SkfB Abstracts a Hydrogen Atom from Cα on SkfA To Initiate Thioether Cross-Link Formation. *Biochemistry 55*, 4131−4134.
(35) Schramma, K. R., Bushin, L. B., and Seyedsayamdost, M. R. (2015) Structure and biosynthesis of a macrocyclic peptide containing an unprecedented lysine-to-tryptophan crosslink. *Nat. Chem. 7*, 431−437.
(36) Blaszczyk, A. J., Wang, B., Silakov, A., Ho, J. V., and Booker, S. J. (2017) Efficient methylation of C2 in L-tryptophan by the cobalamin-dependent radical S-adenosylmethionine methylase TsrM requires an unmodified N1 amine. *J. Biol. Chem. 292*, 15456−15467.
(37) Benjdia, A., Pierre, S., Gherasim, C., Guillot, A., Carmona, M., Amara, P., Banerjee, R., and Berteau, O. (2015) The thiostrepton A tryptophan methyltransferase TsrM catalyses a cob(II)alamin-dependent methyl transfer reaction. *Nat. Commun. 6*, 8377.
(38) Zhang, Z., Mahanta, N., Hudson, G. A., Mitchell, D. A., and Van Der Donk, W. A. (2017) Mechanism of a Class C Radical S-Adenosyl- l -methionine Thiazole Methyl Transferase. *J. Am. Chem. Soc. 139*, 18623−18631.
(39) Mahanta, N., Zhang, Z., Hudson, G. A., Van Der Donk, W. A., and Mitchell, D. A. (2017) Reconstitution and Substrate Specificity of the Radical S-Adenosyl-methionine Thiazole C-Methyltransferase in Thiomuracin Biosynthesis. *J. Am. Chem. Soc. 139*, 4310−4313.
(40) Crone, W. J. K., Leeper, F. J., and Truman, A. W. (2012) Identification and characterisation of the gene cluster for the anti-MRSA antibiotic bottromycin: expanding the biosynthetic diversity of ribosomal peptides. *Chem. Sci. 3*, 3516.
(41) Huo, L., Rachid, S., Stadler, M., Wenzel, S. C., and Müller, R. (2012) Synthetic biotechnology to study and engineer ribosomal bottromycin biosynthesis. *Chem. Biol. 19*, 1278−1287.
(42) Parent, A., Guillot, A., Benjdia, A., Chartier, G., Leprince, J., and Berteau, O. (2016) The B12-Radical SAM Enzyme PoyC Catalyzes Valine Cβ-Methylation during Polytheonamide Biosynthesis. *J. Am. Chem. Soc. 138*, 15515−15518.
(43) Freeman, M. F., Helf, M. J., Bhushan, A., Morinaka, B. I., and Piel, J. (2017) Seven enzymes create extraordinary molecular complexity in an uncultivated bacterium. *Nat. Chem. 9*, 387−395.
(44) Ding, W., Wu, Y., Ji, X., Qianzhu, H., Chen, F., Deng, Z., Yu, Y., and Zhang, Q. (2017) Nucleoside-linked shunt products in the reaction catalyzed by the class C radical S-adenosylmethionine methyltransferase NosN. *Chem. Commun. 53*, 5235−5238.
(45) Bruender, N. A., and Bandarian, V. (2016) The Radical S-Adenosyl- l -methionine Enzyme MftC Catalyzes an Oxidative Decarboxylation of the C-Terminus of the MftA Peptide. *Biochemistry 55*, 2813−2816.
(46) Khaliullin, B., Aggarwal, P., Bubas, M., Eaton, G. R., Eaton, S. S., and Latham, J. A. (2016) Mycofactocin biosynthesis: modification of the peptide MftA by the radical S-adenosylmethionine protein MftC. *FEBS Lett. 590*, 2538−2548.
(47) Khaliullin, B., Ayikpoe, R., Tuttle, M., and Latham, J. A. (2017) Mechanistic elucidation of the mycofactocin-biosynthetic radical S-adenosylmethionine protein, MftC. *J. Biol. Chem. 292*, 13022−13033.
(48) Morinaka, B. I., Vagstad, A. L., Helf, M. J., Gugger, M., Kegler, C., Freeman, M. F., Bode, H. B., and Piel, J. (2014) Radical *S* -Adenosyl Methionine Epimerases: Regioselective Introduction of Diverse D -Amino Acid Patterns into Peptide Natural Products. *Angew. Chem., Int. Ed. 53*, 8503−8507.
(49) Fuchs, S. W., Lackner, G., Morinaka, B. I., Morishita, Y., Asai, T., Riniker, S., and Piel, J. (2016) A Lanthipeptide-like N-Terminal Leader Region Guides Peptide Epimerization by Radical SAM

DOI: 10.1021/acs.biochem.8b00537
Biochemistry 2018, 57, 4816−4823

Epimerases: Implications for RiPP Evolution. *Angew. Chem., Int. Ed. 55*, 12330−12333.
(50) Benjdia, A., Guillot, A., Ruffié, P., Leprince, J., and Berteau, O. (2017) Post-translational modification of ribosomally synthesized peptides by a radical SAM epimerase in Bacillus subtilis. *Nat. Chem. 9*, 698−707.
(51) Morinaka, B. I., Lakis, E., Verest, M., Helf, M. J., Scalvenzi, T., Vagstad, A. L., Sims, J., Sunagawa, S., Gugger, M., and Piel, J. (2018) Natural noncanonical protein splicing yields products with diverse *β*-amino acid residues. *Science (Washington, DC, U. S.) 359*, 779−782.
(52) González-Pastor, J. E. (2011) Cannibalism: a social behavior in sporulating *Bacillus subtilis*. *FEMS Microbiol. Rev. 35*, 415−424.
(53) Suckling, B. C. J. (1988) The Cyclopropyl Group in Studies of Enzyme Mechanism and Inhibition. *Angew. Chem., Int. Ed. Engl. 27*, 537−552.
(54) Spence, E. L., Langley, G. J., and Bugg, T. D. H. (1996) Cis-trans isomerization of a cyclopropyl radical trap catalyzed by extradiol catechol dioxygenases: Evidence for a semiquinone intermediate. *J. Am. Chem. Soc. 118*, 8336−8343.
(55) Shaffer, C. L., Morton, M. D., and Hanzlik, R. P. (2001) Enzymatic N -Dealkylation of an N -Cyclopropylamine: An Unusual Fate for the Cyclopropyl Group. *J. Am. Chem. Soc. 123*, 349−350.
(56) Toy, P. H., Dhanabalasingam, B., Newcomb, M., Hanna, I. H., and Hollenberg, P. F. (1997) A Substituted Hypersensitive Radical Probe for Enzyme-Catalyzed Hydroxylations: Synthesis of Racemic and Enantiomerically Enriched Forms and Application in a Cytochrome P450-Catalyzed Oxidation. *J. Org. Chem. 62*, 9114−9122.
(57) Silverman, R. B., Zhou, J. P., and Eaton, P. E. (1993) Inactivation of monoamine oxidase by (aminomethyl)cubane. First evidence for an.alpha.-amino radical during enzyme catalysis. *J. Am. Chem. Soc. 115*, 8841−8842.
(58) Frey, P. A. (2001) Radical Mechanisms of Enzyme Catalysis. *Annu. Rev. Biochem. 70*, 121−148.
(59) Ruzicka, F., Huang, D. S., Frey, P. A., and Donnelly, M. I. (1990) Methane Monooxygenase Catalyzed Oxygenation of 1,1-Dimethylcyclopropane. Evidence for Radical and Carbocationic Intermediates. *Biochemistry 29*, 1696−1700.
(60) Auclair, K., Hu, Z., Little, D. M., Ortiz de Montellano, P. R., and Groves, J. T. (2002) Revisiting the mechanism of P450 enzymes with the radical clocks norcarane and spiro[2,5]octane. *J. Am. Chem. Soc. 124*, 6020−6027.
(61) Newcomb, M., and Chestney, D. L. (1994) A Hypersensitive Mechanistic Probe for Distinguishing between Radical and Carbocation Intermediates. *J. Am. Chem. Soc. 116*, 9753−9754.
(62) He, M., and Dowd, P. (1998) Mechanism of action of vitamin b12. Ultrafast radical clocks provide no evidence for radical intermediates in cyclopropane models for the methylmalonyl-coa to succinyl-coa carbon skeleton rearrangement. *J. Am. Chem. Soc. 120*, 1133−1137.
(63) Jiang, Y., He, X., and Ortiz De Montellano, P. R. (2006) Radical intermediates in the catalytic oxidation of hydrocarbons by bacterial and human cytochrome P450 enzymes. *Biochemistry 45*, 533−542.
(64) Atkinson, J. K., and Ingold, K. U. (1993) Cytochrome P450 Hydroxylation of Hydrocarbons: Variation in the Rate of Oxygen Rebound Using Cyclopropyl Radical Clocks Including Two New Ultrafast Probes. *Biochemistry 32*, 9209−9214.
(65) Bowry, V. W., Lusztyk, J., and Ingold, K. U. (1991) Calibration of a New Horologery of Fast Radical "Clocks". Ring-Opening Rates for Ring- and *α*-Alkyl-Substituted Cyclopropylcarbinyl Radicals and for the Bicyclo[2.1.0]pent-2-yl Radical. *J. Am. Chem. Soc. 113*, 5687−5698.
(66) Thoden, J. B., and Holden, H. M. (2005) The molecular architecture of human N-acetylgalactosamine kinase. *J. Biol. Chem. 280*, 32784−32791.
(67) Beinert, H. (1983) Semi-micro methods for analysis of labile sulfide and of labile sulfide plus sulfane sulfur in unusually stable iron-sulfur proteins. *Anal. Biochem. 131*, 373−378.
(68) McCarty, R. M., Krebs, C., and Bandarian, V. (2013) Spectroscopic, steady-state kinetic, and mechanistic characterization of the radical SAM enzyme QueE, which catalyzes a complex cyclization reaction in the biosynthesis of 7-deazapurines. *Biochemistry 52*, 188−198.
(69) Bruender, N. A., Young, A. P., and Bandarian, V. (2015) Chemical and biological reduction of the radical SAM enzyme CPH4 synthase. *Biochemistry 54*, 2903−2910.
(70) Lin, G.-M., Choi, S.-H., Ruszczycky, M. W., and Liu, H. (2015) Mechanistic Investigation of the Radical *S* -Adenosyl- l -methionine Enzyme DesII Using Fluorinated Analogues. *J. Am. Chem. Soc. 137*, 4964−4967.

DOI: 10.1021/acs.biochem.8b00537
Biochemistry 2018, 57, 4816−4823